Effects of Viscoelasticity on a Two-Link Filament Model

Michaela Rapier

January 2022

Abstract

De Canio et al. (2017) derived a two-link model to hypothesize how microscopic swimmers move through viscous fluid via flagella beats. My work this summer was attempting to model how viscoelasticity in fluid effects how the same swimmers would move based on the work and model of De Canio et al. (2017) while applying complex fluid stress and strain properties from two different viscoelastic models. The Maxwell model produced a system with a linear analysis that was easy to follow, but its model breaks down when a follower force threshold is surpassed. The Oldroyd-B model produced a more reliable model and a numerical prediction of Hopf bifurcation points.

1 Introduction

The definition of swimming we use comes from Purcell (1976); "...you are in some liquid and are allowed to deform your body in some manner." Cyclic deformations are optimal as they allow an organism to continuously swim. This is seen in microorganisms through flagella and/or cilia, tail or hair like filaments respectively. Flagella and cilia deformation, bending, are caused by dynein motors within and along the filaments. Beats, resulting from the elastic forces of filament binding, molecular motor activity, and the reactions of the surrounding fluid, propel the microorganisms through fluid.

De Canio et al. (2017) established an elastic filament model in viscous fluid with boundary conditions while simplifying the aspects that contribute to the filament's movement by considering a tangential follower force Γ that acts on the tip of the free end of the filament. They then developed a simplified two-link model in viscous fluid with initial conditions including the same follower force. After finding the PDE and ODE systems of equations of motion for both model respectively, linear analysis was conducted.

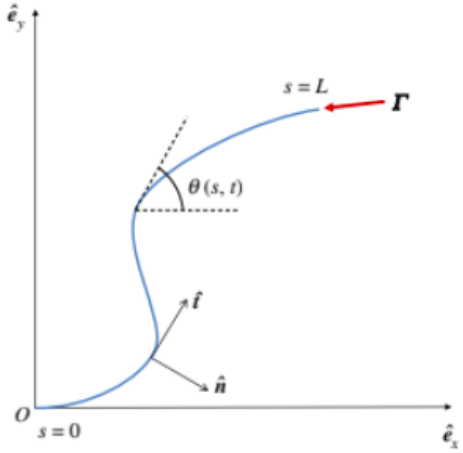

Figure 1: Schematic of the elastic filament clamped at one end with a tangential follower force Γ applied to the end (De Canio et al., 2017). The filament has a length L and arch length $0 \leq s \leq L$. The filament position is defined by $r(s,t)$ or equivalently, by the tangent angle $\theta(s,t)$, providing the clamped end coordinates. $\hat{t}(s,t)$ and $\hat{n}(s,t)$ are the local tangent and unit vectors respectively.

The telling sign for filament oscillation patterns for both models was ω, the eigenvalues of each linearized system set about the resting state (0). Solutions for ω were found in terms of σ in the elastic model and Σ in the two-link

model. The ratio between both is the strength of the follower force (σ) and the elastic force (Σ). The real part of ω represents the growth rate of filament oscillations while the imaginary part of ω represents oscillation frequency. Observing the behavior of both in each model showed that they had similar dynamics. So, we conclude that we can use the two link model (De Canio et al., 2017) in cases with viscoelastic fluid to estimate the viscoelastic effects on an elastic flagella.

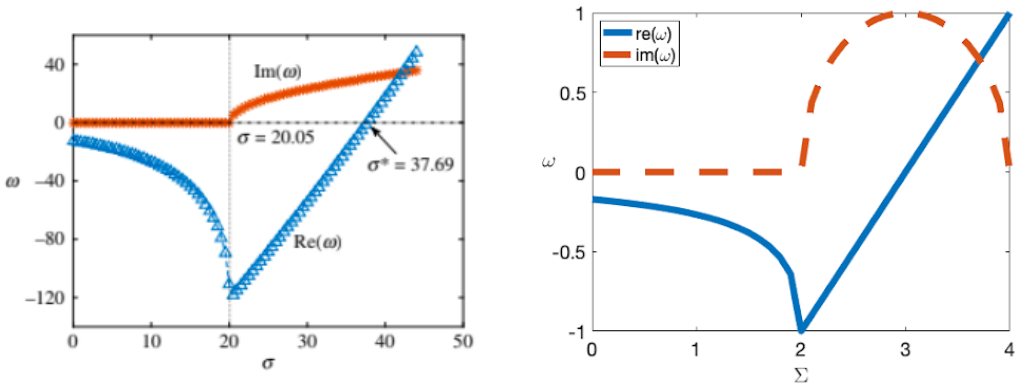

Figure 2: The graphs of the real and imaginary parts of ω in the elastic and two-link models respectively. Similar behavior of both parts in each case hints that the models have similar dynamics.

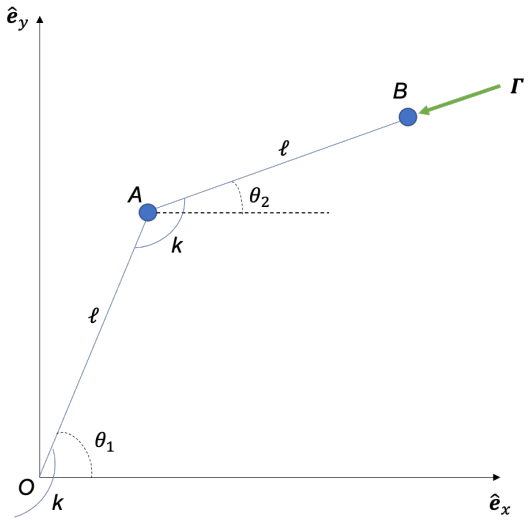

Figure 3: Discrete, two-link model of a filament (similar to De Canio et al., 2017) of two rigid rods of length l, acted on by a follower force, $\mathbf{\Gamma}$, at its tip. The torsional springs at points O and A are of strength k.

As taken from De Canio et al. (2017), our assumptions for the structure of the two-link model we observed in all cases are that, on the plane z = 0, the model is comprised of two rigid links joined together at a point A, with one end clamped at a point O and the other free at a point B. Both links have a length of l. Elasticity is assumed by inducing torsional springs at points O and A, each with the spring constant k. The angles (degrees of freedom) produced at points O and A through elasticity are $\theta_1(t)$ and $\theta_2(t)$. Additionally, both angles are zero when both links are horizontal. Thus, the angles increase counterclockwise. The follower force, Γ, always acts tangentially upon the endpoint of the second link as it moves. Another assumption is that the two-link filament moves in a creeping flow, and its drag force is concentrated at points A and B only. Our final assumptions are that inertia is negligible and damping forces dominate.

The variables that make up the elements in all our calculations are the angles $\theta_1(t)$ and $\theta_2(t)$, which are time-dependent. From these, we can find the locations of the moving points A and B on the model. Then we find the velocities by taking the derivative. The locations are:

$$r_A = A - O = l(\cos\theta_1, \sin\theta_1)$$

and

$$r_B = B - O = l(\cos\theta_1 + \cos\theta_2, \sin\theta_1 + \sin\theta_2)$$

at points A and B respectively. The velocities are:

$$v_A = \dot{r}_A = l\dot{\theta}_1(-\sin\theta_1, \cos\theta_1)$$

and

$$v_B = \dot{r}_B = l[\dot{\theta}_1(-\sin\theta_1, \cos\theta_1) + \dot{\theta}_2(-\sin\theta_2, \cos\theta_2)]$$

at points A and B respectively, and the dots denote time derivatives.

The follower force is scaled as $\Gamma = -\Gamma\hat{t}$, where $\Gamma{>}0$ is the magnitude and $\hat{t} = (cos(\theta_2), sin(\theta_2))$ is the unit tangent vector that joins points A and B.

Because we are assuming creeping flow movement, the drag forces are $F_A = -\zeta(v_A)$ on point A and $F_B = -\zeta(v_B)$ on point B, where ζ is some effective drag force. Finally, the restoring moments (elasticity) of the torsional springs are $-k(\theta_1)$ at point O and $-k(\theta_2 - \theta_1)$ at point A.

2 Viscous Model

In order to understand the mechanics of the two-link model, we first follow the same procedure as De Canio et al. (2017) with a viscous fluid. From there, we will have a template for our cases of interest.

2.1 Derivation and Equations of Motion

We derive the system of ODEs for the two-link filament model in a viscous fluid by asserting the principle of virtual work through the equality

$$\mathbf{\Gamma} \cdot \delta\mathbf{r}_B + \mathbf{F}_B \cdot \delta\mathbf{r}_B + \mathbf{F}_A \cdot \delta\mathbf{r}_A - k\theta_1\delta\theta_1 - k(\theta_1 - \theta_2)(\delta\theta_1 - \delta\theta_2) = 0. \tag{1}$$

We evaluate every individual product in terms of $\theta_1(t)$ and $\theta_2(t)$. We divide the whole equality by k to eliminate the spring constant from the spring restoring moments. Then we nondimensionalize by re-scaling time by $\hat{t} = kt/\zeta l^2$, to cancel out the contained constants, and setting $\Sigma = \Gamma l/k$, the ratio between the follower force and torsional spring constant, to obtain

$$\Sigma\sin(\theta_1 - \theta_2)\delta\theta_1 - (\dot{\theta}_1 + \dot{\theta}_2\cos(\theta_1 - \theta_2))\delta\theta_1 - (\dot{\theta}_2 + \dot{\theta}_1\cos(\theta_1 - \theta_2))\delta\theta_2 - \dot{\theta}_1\delta\theta_1 - \theta_1\delta\theta_1 - (\theta_2 - \theta_1)\delta\theta_2 + (\theta_2 - \theta_1)\delta\theta_1 = 0. \tag{2}$$

Grouping the terms by $\delta\theta_1$ and $\delta\theta_2$, we have

$$[\Sigma\sin(\theta_1 - \theta_2) - (\dot{\theta}_1 + \dot{\theta}_2\cos(\theta_1 - \theta_2) - \dot{\theta}_1 - \theta_1 + (\theta_2 - \theta_1)]\delta\theta_1 + [-(\dot{\theta}_2 + \dot{\theta}_1\cos(\theta_1 - \theta_2)) - (\theta_2 - \theta_1)]\delta\theta_2 = 0. \tag{3}$$

We assume that $\delta\theta_1$ and $\delta\theta_2$ are arbitrary. This produces the system of two equations of motion

$$\Sigma\sin(\theta_1 - \theta_2) - [2\dot{\theta}_1 + \dot{\theta}_2\cos(\theta_1 - \theta_2)] - 2\theta_1 + \theta_2 = 0 \tag{4}$$

$$-\dot{\theta}_1\cos(\theta_1 - \theta_2) - \dot{\theta}_2 + \theta_1 - \theta_2 = 0. \tag{5}$$

2.2 Linear Stability Analysis of Viscous Model

For linear stability analysis of our viscous model, we begin by assuming the equilibrium configuration taken from De Canio et al. (2017); $\theta_1 = \theta_2 = 0$. In other words, the terms are considered to be very small. Also, we assume solutions in the form of $\theta_i = \hat{\theta}_i e^{\omega\tilde{t}}$. A useful note is the approximations for $\sin x$ and $\cos x$ when x is small. We can examine the Taylor series for each at around 0:

$$\sin x = x - \frac{x^3}{3!} + \frac{x^5}{5!} + \cdots$$

$$\cos x = 1 - \frac{x^2}{2!} + \frac{x^4}{4!} + \cdots.$$

So for small x, the linear approximations for $\sin x$ and $\cos x$ are

$$\sin x \approx x \tag{6}$$

$$\cos x \approx 1. \tag{7}$$

So we assume the Taylor series solutions for $\sin x$ and $\cos x$ when x is small.

We start with the system of two equations of motion we derived. After applying the assumptions, and cancelling all the resulting $e^{\omega \tilde{t}}$s, we obtain the linearized system of equations

$$\Sigma(\hat{\theta}_1 - \hat{\theta}_2) - \omega(2\hat{\theta}_1 + \hat{\theta}_2) - 2\hat{\theta}_1 + \hat{\theta}_2 = 0 \tag{8}$$

$$-\omega(\hat{\theta}_1 - \hat{\theta}_2) + \hat{\theta}_1 - \hat{\theta}_2 = 0. \tag{9}$$

Separating the equations by $\hat{\theta}_1$ and $\hat{\theta}_2$ gives a system that can be translated to a matrix linear system:

$$\begin{bmatrix} (\Sigma - 2\omega - 2) & (-\Sigma - \omega + 1) \\ (-\omega + 1) & (-\omega - 1) \end{bmatrix} \begin{bmatrix} \hat{\theta}_1 \\ \hat{\theta}_2 \end{bmatrix} = \begin{bmatrix} 0 \\ 0 \end{bmatrix}.$$

When solving for the determinant and assuming optimal stability at the value zero, we find the equation

$$\omega^2 + 2(3 - \Sigma)\omega + 1 = 0. \tag{10}$$

From the equation's solution,

$$\omega_{\pm} = \Sigma - 3 \pm \sqrt{(\Sigma - 4)(\Sigma - 2)}, \tag{11}$$

we noticed some patterns in the linear model based on the strength of Σ that allowed us to try to make predictions on the stability of the nonlinear viscous model.

1. $0<\Sigma \leq 2$: Since $\omega_{\pm}<0$, the model should show stable exponential decay.
2. $2<\Sigma<3$: $Re(\omega_{\pm})<0$ while $Im(\omega_{\pm}) \neq 0$. Thus the model should show stable decaying oscillations.
3. $\Sigma = 3$: $Re(\omega_{\pm}) = 0$ while $Im(\omega_{\pm}) \neq 0$. thus the model should show stable oscillations with constant amplitude.
4. $3<\Sigma<4$: $Re(\omega_{\pm})>0$ while $Im(\omega_{\pm}) \neq 0$. Thus the model should show growing oscillations. The oscillations would presumably be unstable but that was not clear.
5. $\Sigma \geq 4$: $Re(\omega_{\pm})>0$ while $Im(\omega_{\pm}) = 0$. Thus the model should show unstable exponential growth.

By simulating the changes in both thetas dependent on time and Σ in MatLab using ode45, we saw the linear analysis predictions did not hold true for every Σ value in the nonlinear model. Cases 4 and 5, with values $3<\Sigma<4$ and $\Sigma \geq 4$ respectively, produced self-sustained oscillations as opposed to constantly increasing oscillations or exponential increase.

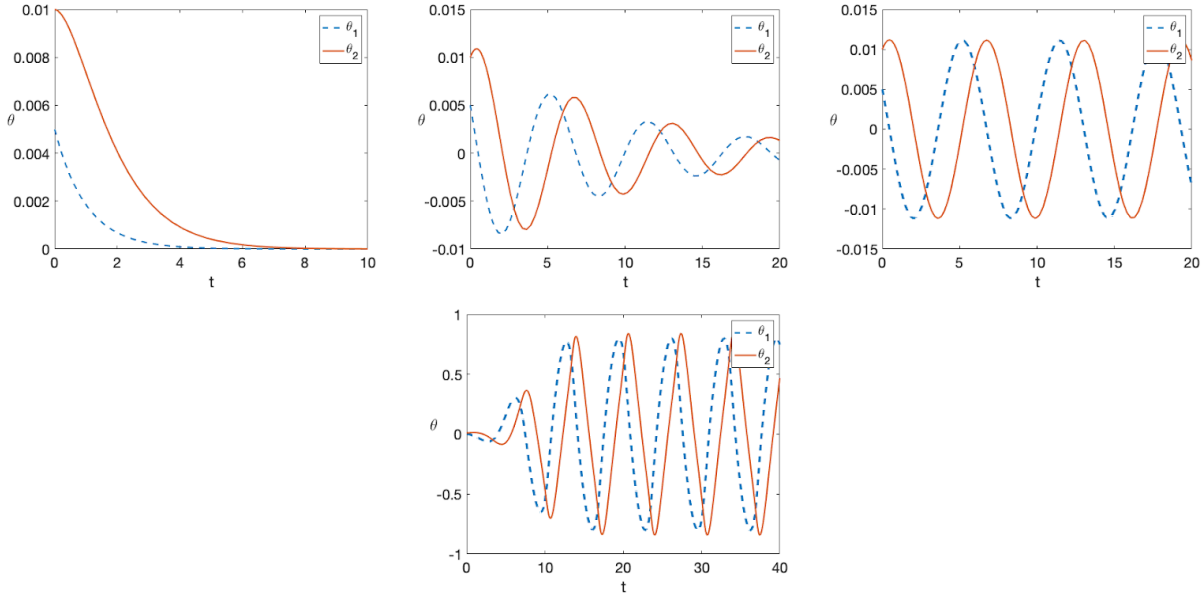

Figure 4: Models of oscillations of two-link filament in viscous fluid at Σ values 2, 2.9, 3, and 3.5 respectively.

3 Adding Viscoelasticity to Two-link filament model

To consider the effects of a viscoelastic fluid on our two-link model, after a viscous only fluid, is to consider complex fluid. In a Newtonian (viscous) fluid, the only internal stresses are due to pressure and viscosity. Viscous stresses in particular have linear deformation rates. Complex, or non-Newtonian fluids are often mixtures that contain polymers, which accounts for some of their elasticity. In comparison to Newtonian fluids, complex fluids have a nonlinear relationship between stress and strain, which causes them to behave differently. These fluids possess properties of fluids and solids. Viscosity, in that it can be used as a measure of resistance to flow, is a fluid property. Viscosity also isn't constant. Elasticity, which gives the fluids the ability to resume is original shape after being deformed, is a solid property. (Özkaya, 2012)

3.1 Equation Modifications

As with the case of viscous fluid, we begin solving for the equation of motion for the two-link model in viscoelastic fluid by considering the equation for the principle of virtual work (De Canio et al., 2017):

$$\mathbf{\Gamma} \cdot \delta \mathbf{r}_B + \mathbf{F}_B \cdot \delta \mathbf{r}_B + \mathbf{F}_A \cdot \delta \mathbf{r}_A - k\theta_1 \delta\theta_1 - k(\theta_1 - \theta_2)(\delta\theta_1 - \delta\theta_2) = 0. \tag{12}$$

We replace the drag forces due to the fluid, $\mathbf{F}_A$, $\mathbf{F}_B$, with a viscoelastic force defined through the Maxwell model defined by Özkaya (2012);

$$\dot{\boldsymbol{\sigma}} + \frac{E}{\eta}\boldsymbol{\sigma} = E\dot{\boldsymbol{\epsilon}}, \tag{13}$$

$$\frac{\eta}{E}\dot{\boldsymbol{\sigma}} + \boldsymbol{\sigma} = \eta\dot{\boldsymbol{\epsilon}}. \tag{14}$$

We define σ as the stress of the fluid, and $\eta\dot{\epsilon}$ as the viscous force. So, after renaming some parameters, we find

$$\lambda\dot{\boldsymbol{\sigma}} + \boldsymbol{\sigma} = \mathbf{F}_{viscous}. \tag{15}$$

From here we can represent $\mathbf{F}_{viscous}$ with the viscous force $-\eta\mathbf{v}$. So,

$$\lambda\dot{\boldsymbol{\sigma}} + \boldsymbol{\sigma} = -\eta\mathbf{v}. \tag{16}$$

Now we use this differential equation to add to our system for the two link model. In this scenario for the Maxwell Model we replace our past drag forces $\mathbf{F}_A$ and $\mathbf{F}_B$ with $\boldsymbol{\sigma}_A$ and $\boldsymbol{\sigma}_B$ respectively. Thus the modified equations of motion are

$$\mathbf{\Gamma} \cdot \delta \mathbf{r}_B + \boldsymbol{\sigma}_B \cdot \delta \mathbf{r}_B + \boldsymbol{\sigma}_A \cdot \delta \mathbf{r}_A - k\theta_1 \delta\theta_1 - k(\theta_1 - \theta_2)(\delta\theta_1 - \delta\theta_2) = 0 \tag{17}$$

$$\lambda\dot{\boldsymbol{\sigma}}_A + \boldsymbol{\sigma}_A = -\eta\mathbf{v}_A \tag{18}$$

$$\lambda\dot{\boldsymbol{\sigma}}_B + \boldsymbol{\sigma}_B = -\eta\mathbf{v}_B. \tag{19}$$

Following from this model we parametrize each σ as (σ_x, σ_y), which produces four different equations accounting for fluid drag forces at the two points A and B. This will yield six equations of motion.

We recall the main equation of motion for this system:

$$\begin{aligned} -\Gamma l\sin(\theta_2 - \theta_1)\delta\theta_1 + l\big(-\sigma_{A_x}\sin\theta_1 + \sigma_{A_y}\cos\theta_1\big)\delta\theta_1 + l[\big(-\sigma_{B_x}\sin\theta_1 + \sigma_{B_y}\cos\theta_1\big)\delta\theta_1 + \\ \big(-\sigma_{B_x}\sin\theta_2 + \sigma_{B_y}\cos\theta_2\big)\delta\theta_2] - k\theta_1\delta\theta_1 - k(\theta_2 - \theta_1)\delta\theta_2 + k(\theta_2 - \theta_1)\delta\theta_1 = 0. \end{aligned} \tag{20}$$

Grouping by $\delta\theta_1$ and $\delta\theta_2$ creates two independent equations.

$$\begin{aligned} \big[-\Gamma l\sin(\theta_2 - \theta_1) + l\big(-\sigma_{A_x}\sin\theta_1 + \sigma_{A_y}\cos\theta_1\big) + l\big(-\sigma_{B_x}\sin\theta_1 + \sigma_{B_y}\cos\theta_1\big) - k\theta_1 + k(\theta_2 - \theta_1)\big]\delta\theta_1 \\ + \big[\big(-\sigma_{B_x}\sin\theta_2 + \sigma_{B_y}\cos\theta_2\big) - k(\theta_2 - \theta_1)\big]\delta\theta_2 = 0. \end{aligned} \tag{21}$$

After accounting for the arbitrariness of $\delta\theta_1$ and $\delta\theta_2$ and expanding the equations for $\boldsymbol{\sigma}$, we obtain the following

initial system of equations:

$$0 = -\Gamma l \sin(\theta_2 - \theta_1) + l\big[-(\sigma_{A_x} + \sigma_{B_x}) \sin\theta_1 + \big(\sigma_{A_y} + \sigma_{B_y}\big) \cos\theta_1\big] + k(\theta_2 - 2\theta_1) \tag{22}$$

$$0 = l\big[-\sigma_{B_x} \sin\theta_2 + \sigma_{B_y} \cos\theta_2\big] - k(\theta_2 - \theta_1) \tag{23}$$

$$\lambda\dot{\sigma}_{A_x} + \sigma_{A_x} = \zeta l\dot{\theta}_1 \sin\theta_1 \tag{24}$$

$$\lambda\dot{\sigma}_{A_y} + \sigma_{A_y} = -\zeta l\dot{\theta}_1 \cos\theta_1 \tag{25}$$

$$\lambda\dot{\sigma}_{B_x} + \sigma_{B_x} = \zeta l\Big(\dot{\theta}_1 \sin\theta_1 + \dot{\theta}_2 \sin\theta_2\Big) \tag{26}$$

$$\lambda\dot{\sigma}_{B_y} + \sigma_{B_y} = -\zeta l\Big(\dot{\theta}_1 \cos\theta_1 + \dot{\theta}_2 \cos\theta_2\Big). \tag{27}$$

We notice that the system of equations of motion is a DAE (Differential Algebraic System of Equations) with four differential equations and two constraint equations.

3.2 Linearization

We linearize the above system about $\theta_1 = \theta_2 = 0$ once again. We also assume that, along with θ_1 and θ_2, σ_{A_x}, σ_{A_y}, σ_{B_x}, and σ_{B_y} are small. We also apply the Taylor series for $\sin x$ and $\cos x$ when x is small again,

Following these assumptions, then regarding the higher order terms as arbitrary gives us

$$0 = -\Gamma l(\theta_2 - \theta_1) + l(\sigma_{A_x} + \sigma_{B_x}) + k(\theta_2 - 2\theta_1) \tag{28}$$

$$0 = l\sigma_{B_y} - k(\theta_2 - \theta_1) \tag{29}$$

$$\lambda\dot{\sigma}_{A_x} + \sigma_{A_x} = 0 \tag{30}$$

$$\lambda\dot{\sigma}_{A_y} + \sigma_{A_y} = -\zeta l\dot{\theta}_1 \tag{31}$$

$$\lambda\dot{\sigma}_{B_x} + \sigma_{B_x} = 0 \tag{32}$$

$$\lambda\dot{\sigma}_{B_y} + \sigma_{B_y} = -\zeta l\Big(\dot{\theta}_1 + \dot{\theta}_2\Big). \tag{33}$$

Since σ_{A_x} and σ_{B_x} are small, we approximate them both to be zero. Thus our linearized system of equations is

$$0 = -\Gamma l(\theta_2 - \theta_1) + l(\sigma_{A_x} + \sigma_{B_x}) + k(\theta_2 - 2\theta_1) \tag{34}$$

$$0 = l\sigma_{B_y} - k(\theta_2 - \theta_1) \tag{35}$$

$$\lambda\dot{\sigma}_{A_y} + \sigma_{A_y} = -\zeta l\dot{\theta}_1 \tag{36}$$

$$\lambda\dot{\sigma}_{B_y} + \sigma_{B_y} = -\zeta l\Big(\dot{\theta}_1 + \dot{\theta}_2\Big). \tag{37}$$

3.3 Nondimensionalization

To nondimensionalize the linearized system, we scale t, σ, and θ, using the substitutions

$$t = T\hat{t},\ \sigma = \tilde{\Sigma}\hat{\sigma}, \text{ and } \theta = \alpha\hat{\theta},$$

for some scaling factors T, $\tilde{\Sigma}$, and α. Making these substitutions gives us

$$-\Gamma l\alpha(\hat{\theta}_2 - \hat{\theta}_1) + l\tilde{\Sigma}(\hat{\sigma}_{A_y} + \hat{\sigma}_{B_y}) + k\alpha(\hat{\theta}_1 - 2\hat{\theta}_2) = 0 \tag{38}$$

$$l\tilde{\Sigma}\hat{\sigma}_{B_y} - k\alpha(\hat{\theta}_2 - \hat{\theta}_1) = 0 \tag{39}$$

$$\lambda\tilde{\Sigma}\frac{1}{T}\dot{\hat{\sigma}}_{A_y} + \tilde{\Sigma}\hat{\sigma}_{A_y} = -\zeta l\alpha\frac{1}{T}\dot{\hat{\theta}}_1 \tag{40}$$

$$\lambda\tilde{\Sigma}\frac{1}{T}\dot{\hat{\sigma}}_{B_y} + \tilde{\Sigma}\hat{\sigma}_{B_y} = -\zeta l\alpha\frac{1}{T}(\dot{\hat{\theta}}_1 + \dot{\hat{\theta}}_2). \tag{41}$$

Note that we have chosen the parameters of interest so that they are related to the follower force, Γ, and the fluid relaxation time, λ. Dividing in the first two equations by $k\alpha$ allows us to relate the strength of the follower force to the strength of the torsional springs at θ_1 and θ_2, as De Canio et al. (2017) had done. Likewise, dividing in the

last two equations by $\tilde{\Sigma}$ allows us to relate the fluid relaxation time, λ, to the mechanical relaxation time, T. These steps result in the system

$$-\frac{\Gamma l}{k}(\hat{\theta}_2 - \hat{\theta}_1) + \frac{l\tilde{\Sigma}}{k\alpha}(\hat{\sigma}_{A_y} + \hat{\sigma}_{B_y}) + (\hat{\theta}_1 - 2\hat{\theta}_2) = 0 \tag{42}$$

$$\frac{l\tilde{\Sigma}}{k\alpha}\hat{\sigma}_{B_y} - (\hat{\theta}_2 - \hat{\theta}_1) = 0 \tag{43}$$

$$\lambda\frac{1}{T}\dot{\hat{\sigma}}_{A_y} + \hat{\sigma}_{A_y} = -\frac{\zeta l\alpha}{\tilde{\Sigma}}\frac{1}{T}\dot{\hat{\theta}}_1 \tag{44}$$

$$\lambda\frac{1}{T}\dot{\hat{\sigma}}_{B_y} + \hat{\sigma}_{B_y} = -\frac{\zeta l\alpha}{\tilde{\Sigma}}\frac{1}{T}(\dot{\hat{\theta}}_1 + \dot{\hat{\theta}}_2). \tag{45}$$

Setting $\tilde{\Sigma} = \frac{k\alpha}{l}$ would cancel out the respective coefficients in the first two equations. Regarding the last two equation, we have a choice to either express T in terms of λ, or as $\frac{\zeta l^2}{k}$. Since we are interested in a parameter that relates to fluid relaxation time, we want to be able to freely manipulate λ. Thus, we choose $T = \frac{\zeta l^2}{k}$. We also set $\Sigma = \frac{\Gamma l}{k}$ (equivalent to before) and $\Lambda = \frac{k\lambda}{\zeta l^2}$. With all these parameters together, we obtain

$$\Sigma(\hat{\theta}_1 - \hat{\theta}_2) + (\hat{\sigma}_{A_y} + \hat{\sigma}_{B_y}) + (\hat{\theta}_1 - 2\hat{\theta}_2) = 0 \tag{46}$$

$$\hat{\sigma}_{B_y} - (\hat{\theta}_2 - \hat{\theta}_1) = 0 \tag{47}$$

$$\Lambda\dot{\hat{\sigma}}_{A_y} + \hat{\sigma}_{A_y} = -\dot{\hat{\theta}}_1 \tag{48}$$

$$\Lambda\dot{\hat{\sigma}}_{B_y} + \hat{\sigma}_{B_y} = -(\dot{\hat{\theta}}_1 + \dot{\hat{\theta}}_2). \tag{49}$$

as our nondimensionalized linear system.

3.3.1 Nonlinear System

Using the same scaling factors from the linear system, we establish an official nonlinear system of equations of motion:

$$0 = -\Sigma\sin(\theta_2 - \theta_1) - (\sigma_{A_x} + \sigma_{B_x})\sin\theta_1 + \left(\sigma_{A_y} + \sigma_{B_y}\right)\cos\theta_1 + \theta_2 - 2\theta_1 \tag{50}$$

$$0 = -\sigma_{B_x}\sin\theta_2 + \sigma_{B_y}\cos\theta_2 - \theta_2 + \theta_1 \tag{51}$$

$$\Lambda\dot{\sigma}_{A_x} + \sigma_{A_x} = \dot{\theta}_1\sin\theta_1 \tag{52}$$

$$\Lambda\dot{\sigma}_{A_y} + \sigma_{A_y} = -\dot{\theta}_1\cos\theta_1 \tag{53}$$

$$\Lambda\dot{\sigma}_{B_x} + \sigma_{B_x} = \left(\dot{\theta}_1\sin\theta_1 + \dot{\theta}_2\sin\theta_2\right) \tag{54}$$

$$\Lambda\dot{\sigma}_{B_y} + \sigma_{B_y} = -\left(\dot{\theta}_1\cos\theta_1 + \dot{\theta}_2\cos\theta_2\right). \tag{55}$$

The nonlinear system was converted to the form $My' = f(y)$, where

$$M = \begin{bmatrix} \Lambda & 0 & 0 & 0 & -sin(\theta_1) & 0 \\ 0 & \Lambda & 0 & 0 & cos(\theta_1) & 0 \\ 0 & 0 & \Lambda & 0 & -sin(\theta_1) & -sin(\theta_2) \\ 0 & 0 & 0 & \Lambda & cos(\theta_1) & cos(\theta_2) \\ 0 & 0 & 0 & 0 & 0 & 0 \\ 0 & 0 & 0 & 0 & 0 & 0 \end{bmatrix}, y' = \begin{bmatrix} \dot{\sigma}_{A_x} \\ \dot{\sigma}_{A_y} \\ \dot{\sigma}_{B_x} \\ \dot{\sigma}_{B_y} \\ \dot{\theta}_1 \\ \dot{\theta}_2 \end{bmatrix}.$$

This system was modeled in MatLab using ode15s. We noticed that fluid elasticity changes oscillation patterns for fixed Σ values.

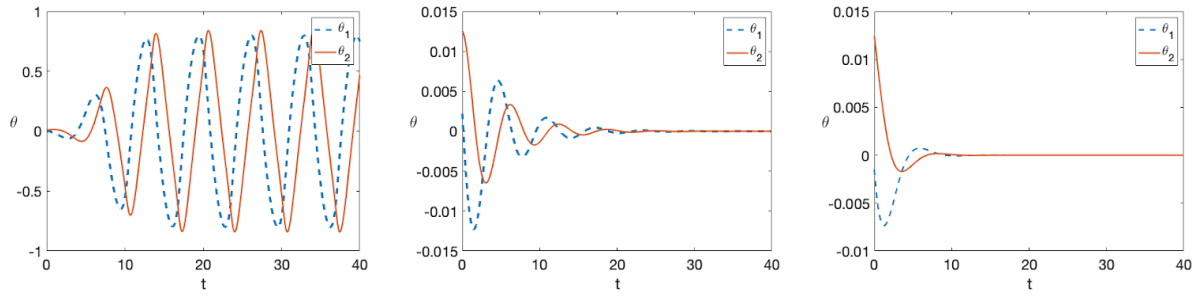

Figure 5: Models of oscillations of two-link filament in viscoelastic fluid at $\Sigma = 3.3$ and Λ values 0, 0.5, and 1 respectively.

3.4 Linear Stability Analysis of Viscoelastic Model

Using the nondimensionalized linear system for the viscoelastic model, we assume solutions of the form $\theta_j = \hat{\theta}_j e^{\omega \hat{t}}$, as in the viscous model, and $\sigma_j = \hat{\sigma}_j e^{\omega \hat{t}}$. This results in the system

$$\Sigma(\hat{\theta}_1 - \hat{\theta}_2) + (\hat{\sigma}_{A_y} + \hat{\sigma}_{B_y}) + (\hat{\theta}_1 - 2\hat{\theta}_2) = 0 \tag{56}$$

$$\hat{\sigma}_{B_y} - (\hat{\theta}_2 - \hat{\theta}_1) = 0 \tag{57}$$

$$\Lambda\omega\hat{\sigma}_{A_y} + \hat{\sigma}_{A_y} = -\omega\hat{\theta}_1 \tag{58}$$

$$\Lambda\omega\hat{\sigma}_{B_y} + \hat{\sigma}_{B_y} = -(\omega\hat{\theta}_1 + \omega\hat{\theta}_2). \tag{59}$$

By separating these equations by $\hat{\theta}_1$, $\hat{\theta}_2$, $\hat{\sigma}_{A_y}$, and $\hat{\sigma}_{B_y}$, the system can be translated into the following matrix equation:

$$\begin{bmatrix} (\Sigma-2) & (-\Sigma+1) & 1 & 1 \\ 1 & -1 & 0 & 1 \\ \omega & 0 & (\Lambda\omega+1) & 0 \\ \omega & \omega & 0 & (\Lambda\omega+1) \end{bmatrix} \begin{bmatrix} \hat{\theta}_1 \\ \hat{\theta}_2 \\ \hat{\sigma}_{A_y} \\ \hat{\sigma}_{B_y} \end{bmatrix} = \begin{bmatrix} 0 \\ 0 \\ 0 \\ 0 \end{bmatrix}.$$

By once again assuming optimal stability at the value zero when solving for the determinant, we find the equation

$$(-2\Sigma\Lambda + \Lambda^2 + 6\Lambda + 1)\omega^2 + (-2\Sigma + 2\Lambda + 6)\omega + 1 = 0, \tag{60}$$

which has the solution

$$\omega_{\pm} = \frac{\Sigma - \Lambda - 3 \pm \sqrt{(\Sigma-4)(\Sigma-2)}}{-2\Sigma\Lambda + \Lambda^2 + 6\Lambda + 1}.. \tag{61}$$

Note that when $\Lambda = 0$, $\omega_{\pm}$ is the same as the viscous model for all values of Σ.

3.5 Finding Hopf Bifurcation Points and Predicting Oscillation Frequency of Viscoelastic Model

To better predict the frequency of the filament oscillations for the viscoelastic model, we can narrow down the linear stability to its Hopf bifurcation point. In other words, we bring the real part of $\omega_{\pm}$, which represents the exponential growth or decay of the oscillations, to zero so that we can isolate the imaginary part, the frequency.

Recalling our solution for $\omega_{\pm}$, the square root is the origin of ω's imaginary part. Observing the factor product within the root, we establish a preliminary boundary for Σ concerning the frequency of oscillations and the Hoph bifurcation points:

$$2 < \Sigma < 4.$$

The real part is the numerator equation sans the square root. Because the real part must be zero, we can algebraically determine the value of Σ at the bifurcation point dependent on Λ,

$$Re(\omega_{\pm}) = \Sigma - \Lambda - 3 = 0 \Rightarrow \Sigma = \Lambda + 3$$

Recall that $\Lambda = \frac{k\lambda}{\zeta l^2}$. λ represents the relaxation time of our viscoelastic fluid. So, Λ cannot be negative: $\Lambda > 0$. Applying this to the boundaries of Σ changes the minimum from 2 to 3:

$$3 < \Sigma < 4 \Rightarrow 3 < \Lambda + 3 < 4 \Rightarrow 0 < \Lambda < 1$$

Therefore, the bifurcation boundaries for Σ and Λ are $3 < \Sigma < 4$ and $0 < \Lambda < 1$.

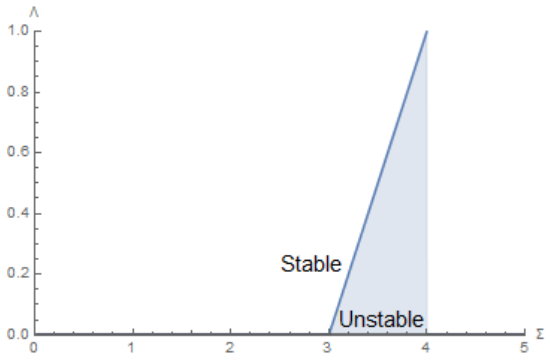

Figure 6: Here we see a linear relationship between the bifurcation point Σ with Λ varying from 0 to 1.

We can predict the frequency at the bifurcation point by substituting Σ in terms of Λ in the $\omega_{\pm}$ solution, then graphing the imaginary part with a varying Λ.

$$\omega_{\pm} = \frac{0 \pm \sqrt{(\Lambda - 1)(\Lambda + 1)}}{-\Lambda^2 + 1} \tag{62}$$

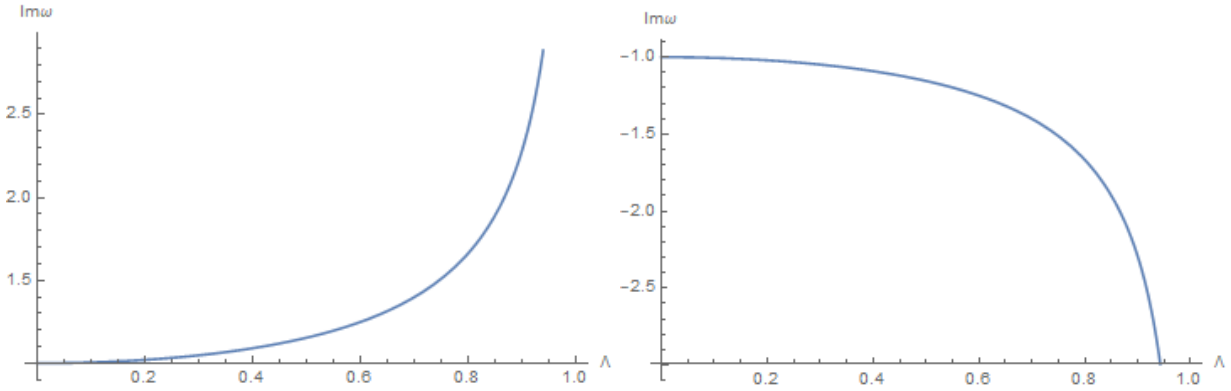

Figure 7: The graphs of the imaginary parts, i.e. the frequency of oscillations, ω_+ and ω_- respectively, show exponential relationships with Λ varying from 0 to 1.

3.6 Considering Another Viscoelastic Model

Unfortunately, following the Maxwell viscoelastic model led to a breakdown in the numerical solution obtained using MatLab. When we choose a Σ value greater than 3.3, the oscillations become uneven and do not follow the growth rate and frequency patterns we noticed beforehand. Also, by choosing any Λ value greater than 0, we transition from a purely viscous fluid to a purely viscoelastic fluid. We wanted to observe the effects the fluid would have on the filament as we smoothly transition between the two. So, we decided to rework the equations of motion from scratch by considering a different viscoelastic model for a basis.

4 Oldroyd-B Model

4.1 Model Derivation

We use the Oldroyd-B model to create a viscoelastic model that considers the total viscosity, ζ, as a sum of the fluid viscosity, ζ_f, and polymeric viscosity, ζ_p. We apply this to the principal of virtual work by adding the viscous fluid drag force terms from the viscous model into to the Maxwell model. The resulting basis for the Oldroyd-B model is

$$\mathbf{\Gamma} \cdot \delta\mathbf{r}_B + \mathbf{F}_B \cdot \delta\mathbf{r}_B + \sigma_B \cdot \delta\mathbf{r}_B + \mathbf{F}_A \cdot \delta\mathbf{r}_A + \sigma_B \cdot \delta\mathbf{r}_B - k\theta_1\delta\theta_1 - k(\theta_1 - \theta_2)(\delta\theta_1 - \delta\theta_2) = 0. \tag{63}$$

Expanding From this equation we obtain

$$-\Gamma l\sin(\theta_2-\theta_1)-\zeta l^2[(\dot\theta_1+\dot\theta_2\cos(\theta_1-\theta_2))\delta\theta_1+(\dot\theta_2+\dot\theta_1\cos(\theta_1-\theta_2))\delta\theta_2]+l\delta\theta_1(-\sin\theta_1\sigma_{B_x}+\cos\theta_1\sigma_{B_y})$$
$$+l\delta\theta_2(-\sin\theta_2\sigma_{B_x}+cos\theta_2\sigma_{B_y})-\zeta l^2\dot\theta_1\delta\theta_1+l\delta\theta_1(-\sin\theta_1\sigma_{A_x}+\cos\theta_1\sigma_{A_y})-k\theta_1\delta\theta_1-k(\theta_2-\theta_1)\delta\theta_2+k(\theta_2-\theta_1)\delta\theta_1=0. \tag{64}$$

Due to the arbitrariness of $\delta\theta_1$ and $\delta\theta_2$, and combining our viscoelastic equations from the Maxwell model, we again obtain a system of six equations:

$$0=-\Gamma l\sin(\theta_2-\theta_1)+l(-\sin\theta_1(\sigma_{A_x}+\sigma_{B_x})+\cos\theta_1(\sigma_{A_y}+\sigma_{B_y}))-2\zeta_f l^2\dot\theta_1-\zeta_f l^2\dot\theta_2\cos(\theta_1-\theta_2)-2k\theta_1+k\theta_2 \tag{65}$$

$$0=l(-\sin\theta_2\sigma_{B_x}+\cos\theta_2\sigma_{B_y})-\zeta_f l^2(\dot\theta_2+\dot\theta_1\cos(\theta_1-\theta_2))-k(\theta_2-\theta_1) \tag{66}$$

$$\lambda\dot\sigma_{A_x}+\sigma_{A_x}=\zeta_p l\dot\theta_1\sin\theta_1 \tag{67}$$

$$\lambda\dot\sigma_{A_y}+\sigma_{A_y}=-\zeta_p l\dot\theta_1\cos\theta_1 \tag{68}$$

$$\lambda\dot\sigma_{B_x}+\sigma_{B_x}=\zeta_p l\Big(\dot\theta_1\sin\theta_1+\dot\theta_2\sin\theta_2\Big) \tag{69}$$

$$\lambda\dot\sigma_{B_y}+\sigma_{B_y}=-\zeta_p l\Big(\dot\theta_1\cos\theta_1+\dot\theta_2\cos\theta_2\Big). \tag{70}$$

4.2 Linearization

Linearizing using the same method as the Maxwell model yields the linear system

$$0=-\Gamma l(\theta_2-\theta_1)+l(\sigma_{A_y}+\sigma_{B_y})-2\zeta_p l^2\dot\theta_1-\zeta_p l^2\dot\theta_2+k(\theta_2-2\theta_1) \tag{71}$$

$$0=l\sigma_{B_y}-\zeta_p l^2(\dot\theta_2+\dot\theta_1)-k(\theta_2-\theta_1) \tag{72}$$

$$\lambda\dot\sigma_{A_y}+\sigma_{A_y}=-\zeta_p l\dot\theta_1 \tag{73}$$

$$\lambda\dot\sigma_{B_y}+\sigma_{B_y}=-\zeta_p l\Big(\dot\theta_1+\dot\theta_2\Big). \tag{74}$$

4.3 Nondimensionalization

We nondimensionalize using the same scaling factors: $t=T\hat t$, $\sigma=\tilde\Sigma\hat\sigma$, and $\theta=\alpha\hat\theta$. Substituting these terms gives us

$$0=-\Gamma l\alpha(\hat\theta_2-\hat\theta_1)+l\tilde\Sigma(\hat\sigma_{A_y}+\hat\sigma_{B_y})-2\frac{\zeta_p l^2\alpha}{T}\dot{\hat\theta}_1-\frac{\zeta_p l^2\alpha}{T}\dot{\hat\theta}_2+k\alpha(\hat\theta_2-2\hat\theta_1) \tag{75}$$

$$0=l\tilde\Sigma\hat\sigma_{B_y}-\frac{\zeta_p l^2\alpha}{T}(\dot{\hat\theta}_2+\dot{\hat\theta}_1)-k\alpha(\hat\theta_2-\hat\theta_1) \tag{76}$$

$$\frac{\lambda\tilde\Sigma}{T}\dot{\hat\sigma}_{A_y}+\tilde\Sigma\hat\sigma_{A_y}=-\frac{\zeta_p l\alpha}{T}\dot{\hat\theta}_1 \tag{77}$$

$$\frac{\lambda\tilde\Sigma}{T}\dot{\hat\sigma}_{B_y}+\tilde\Sigma\hat\sigma_{B_y}=-\frac{\zeta_p l\alpha}{T}(\dot{\hat\theta}_1+\dot{\hat\theta}_2). \tag{78}$$

We again divide the first two equations by $k\alpha$ and the last two by $\tilde\Sigma$ to obtain

$$0=-\frac{\Gamma l}{k}(\hat\theta_2-\hat\theta_1)+\frac{l\tilde\Sigma}{k\alpha}(\hat\sigma_{A_y}+\hat\sigma_{B_y})-2\frac{\zeta_p l^2}{kT}\dot{\hat\theta}_1-\frac{\zeta_p l^2}{kT}\dot{\hat\theta}_2+(\hat\theta_2-2\hat\theta_1) \tag{79}$$

$$0=\frac{l\tilde\Sigma}{k\alpha}\hat\sigma_{B_y}-\frac{\zeta_p l^2}{kT}(\dot{\hat\theta}_2+\dot{\hat\theta}_1)-(\hat\theta_2-\hat\theta_1) \tag{80}$$

$$\frac{\lambda}{T}\dot{\hat\sigma}_{A_y}+\hat\sigma_{A_y}=-\frac{\zeta_p l\alpha}{\tilde\Sigma T}\dot{\hat\theta}_1 \tag{81}$$

$$\frac{\lambda}{T}\dot{\hat\sigma}_{B_y}+\hat\sigma_{B_y}=-\frac{\zeta_p l\alpha}{\tilde\Sigma T}(\dot{\hat\theta}_1+\dot{\hat\theta}_2). \tag{82}$$

Making the substitutions $\tilde{\Sigma} = \frac{k\alpha}{l}$, $T = \frac{(\zeta_f+\zeta_p)l^2}{k}$, $\Sigma = \frac{\Gamma l}{k}$, $\Lambda = \frac{k\lambda}{\zeta_f l^2}$, and $\beta = \frac{\zeta_p}{\zeta_f+\zeta_p}$ to account for both fluid and polymer viscosity, we find the nondimensional linear system

$$0 = \Sigma(\theta_1 - \theta_2) + \sigma_{A_y} + \sigma_{B_y} - 2(1-\beta)\dot{\theta}_1 - (1-\beta)\dot{\theta}_2 + \theta_2 - 2\theta_1 \tag{83}$$

$$0 = \sigma_{B_y} - (1-\beta)(\dot{\theta}_2 + \dot{\theta}_1) - \theta_2 + \theta_1 \tag{84}$$

$$\Lambda\dot{\sigma}_{A_y} + \sigma_{A_y} = -\beta\dot{\theta}_1 \tag{85}$$

$$\Lambda\dot{\sigma}_{B_y} + \sigma_{B_y} = -\beta(\dot{\theta}_1 + \dot{\theta}_2). \tag{86}$$

4.4 Nonlinear system

By applying the same scaling factors to the nonlinear system, we obtain the following system of equations of motion:

$$0 = \Sigma\sin(\theta_1 - \theta_2) - \sin\theta_1(\sigma_{A_x} + \sigma_{B_x}) + \cos\theta_1(\sigma_{A_y} + \sigma_{B_y}) - 2(1-\beta)\dot{\theta}_1 - (1-\beta)\dot{\theta}_2\cos(\theta_1 - \theta_2) - 2\theta_1 + \theta_2 \tag{87}$$

$$0 = -\sin\theta_2\sigma_{B_x} + \cos\theta_2\sigma_{B_y} - (1-\beta)(\dot{\theta}_2 + \dot{\theta}_1\cos(\theta_1 - \theta_2)) - \theta_2 + \theta_1 \tag{88}$$

$$\Lambda\dot{\sigma}_{A_x} + \sigma_{A_x} = \beta\dot{\theta}_1\sin\theta_1 \tag{89}$$

$$\Lambda\dot{\sigma}_{A_y} + \sigma_{A_y} = -\beta\dot{\theta}_1\cos\theta_1 \tag{90}$$

$$\Lambda\dot{\sigma}_{B_x} + \sigma_{B_x} = \beta(\dot{\theta}_1\sin\theta_1 + \dot{\theta_2}\sin\theta_2) \tag{91}$$

$$\Lambda\dot{\sigma}_{B_y} + \sigma_{B_y} = -\beta(\dot{\theta}_1\cos\theta_1 + \dot{\theta_2}\cos\theta_2). \tag{92}$$

4.5 Stability Analysis

4.5.1 Linear Analysis Attempt

Again, assuming the solutions $\theta_j = \hat{\theta}_j e^{\omega\hat{t}}$ and $\sigma_j = \hat{\sigma}_j e^{\omega\hat{t}}$, we work through the nondimensionalized linear system of the Oldroyd-B model and find the system

$$\Sigma(\hat{\theta}_1 - \hat{\theta}_2) + \hat{\sigma}_{A_y} + \hat{\sigma}_{B_y} - \omega(1-\beta)(2\hat{\theta}_1 + \hat{\theta}_2) + \hat{\theta}_2 - 2\hat{\theta}_1 = 0 \tag{93}$$

$$\hat{\sigma}_{B_y} - \omega(1-\beta)(\hat{\theta}_2 + \hat{\theta}_1) - \hat{\theta}_2 + \hat{\theta}_1 = 0 \tag{94}$$

$$\omega\Lambda\hat{\sigma}_{A_y} + \hat{\sigma}_{A_y} + \omega\beta\hat{\theta}_1 = 0 \tag{95}$$

$$\omega\Lambda\hat{\sigma}_{B_y} + \hat{\sigma}_{B_y} + \omega\beta(\hat{\theta}_1 + \omega\hat{\theta}_2). \tag{96}$$

We separate the equations by $\hat{\theta}_1$, $\hat{\theta}_2$, $\hat{\sigma}_{A_y}$, and $\hat{\sigma}_{B_y}$, then can translate the system into a matrix equation:

$$\begin{bmatrix} (\Sigma - 2\omega(1-\beta) - 2) & (-\Sigma - \omega(1-\beta) + 1) & 1 & 1 \\ -\omega(1-\beta) + 1 & -\omega(1-\beta) - 1 & 0 & 1 \\ \omega\beta & 0 & (\omega\Lambda + 1) & 0 \\ \omega\beta & \omega\beta & 0 & (\omega\Lambda + 1) \end{bmatrix} \begin{bmatrix} \hat{\theta}_1 \\ \hat{\theta}_2 \\ \hat{\sigma}_{A_y} \\ \hat{\sigma}_{B_y} \end{bmatrix} = \begin{bmatrix} 0 \\ 0 \\ 0 \\ 0 \end{bmatrix}.$$

4.5.2 Numerical Hoph Bifurcation Solutions

Trying solve for the Hoph bifurcation points as solutions for ω individually by finding the determinant like before is a lengthy and complex process. Therefore, we choose to solve for the solutions numerically.

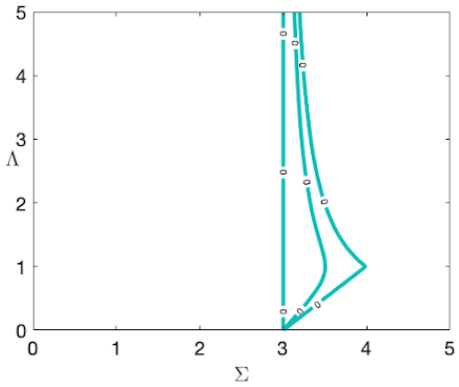

Figure 8: Graph of linear Hoph bifurcation solutions for Λ dependent on Σ and β based on numerical simulation. The vertical bifurcation curve is set for $\beta = 0$, which is equivalent to the viscous case. The middle curve is set for $\beta = 0.67$. The most radical curve is set for $\beta = 0.99$, which is equivalent to the Maxwell model case.

Based on the previous analysis we've done in the previous cases, we establish that the Λ coordinates within $0<\Sigma \leq 3$ are stable, while the ones within $3<\Sigma$ are unstable. With this in mind, we notice that as Λ, fluid relaxation rate and strength of viscoelasticity, increases, oscillations stabilize.

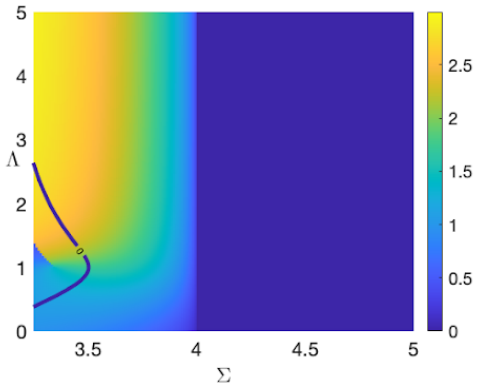

Figure 9: Contour plot of oscillation frequency overlaid with bifurcation curve for $\beta = 0.67$.

With stability in mind, the oscillation frequency contour plot paired with the bifurcation curve for $\beta = 0.67$ reveals two bifurcation points along a fixed example of Σ, $\Sigma = 3.25$. These are $\Lambda \approx 0.4$, which seems to have a moderate frequency, and $\Lambda \approx 2.65$, which seems to have a high frequency.

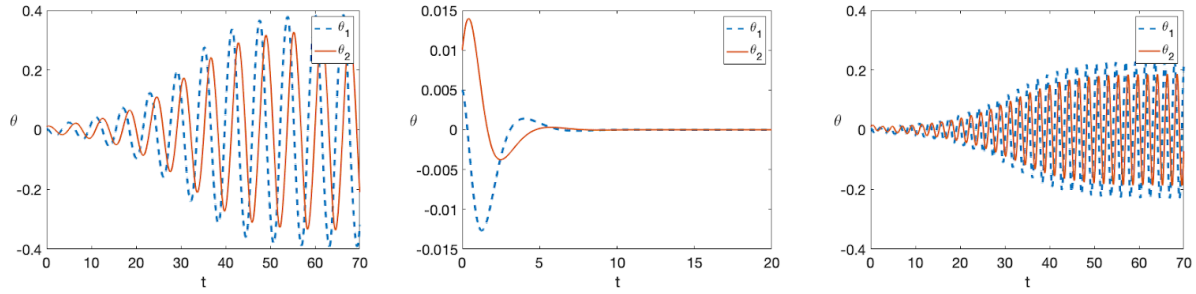

Figure 10: Models of oscillations of a two-link filament in viscoelastic fluid at $\beta = 0.67$, $\Sigma = 3.25$ and Λ values 0.25, 1, and 3 respectfully.

With these points in mind, we are able to establish patterns in oscillation frequency and amplitude for varying

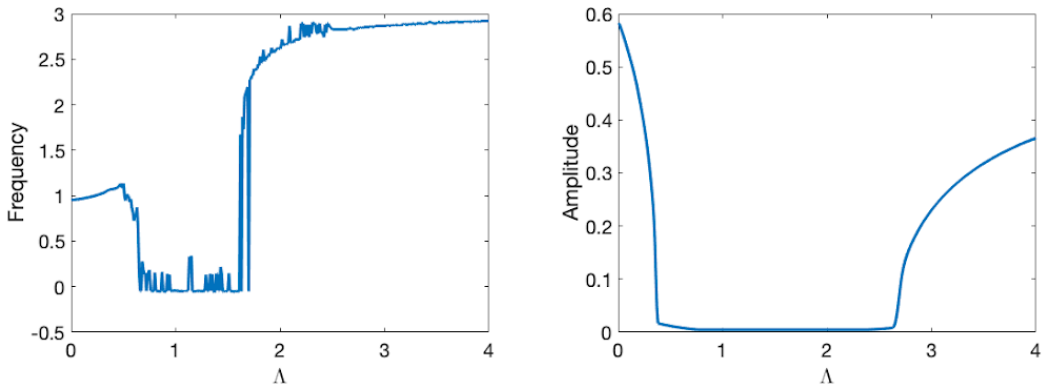

Figure 11: Graphs of the frequency and amplitude of oscillations of the two-link filament Oldroyd-B model with varying Λ and $\beta = 0.67$ and $\Sigma = 3.25$.

values of Λ. Frequency seems moderate when viscoelasticity is low. But once the first bifurcation point is passed, oscillation seems to die out over time, as linear theory predicts. Then frequency seems to spike in strength until it begins increasing at a more gradual rate after passing the second bifurcation point. Amplitude shows similar patterns except it doesn't seem to increase until it passes the second point.

5 Conclusion

Before tackling our main interest, we confirmed that the dynamics of the motions of an elastic filament are similar to the two-link model by De Canio et al. (2017), both in a viscous fluid, and practicing how to build our own two-link model in MatLab following the same derivations. After understanding how to observe the two-links' oscillations, we attempted to modify the equations of motion to a viscoelastic, or complex, fluid.

Using the Maxwell Model as a basis, we observed that greater fluid relaxation time, or strength of elasticity dampens the oscillations of the two-link model. Unfortunately, this model broke down when we tried to run the code with a Σ value greater than 3.3. To see around this, and to better see the effects when we transition from a viscous fluid to a viscoelastic fluid, we created a new model with the Oldroyd-B model as a basis. Numerical analysis on the equations of motion of the Oldroyd-B model revealed two Hoph bifurcation points as opposed to just one with a linear dependence on elasticity. Based on numerical analysis with varying values of β, Σ, and Λ, we realized that viscoelasticity stabilizes oscillating filaments. We found that increased fluid relaxation time decreases oscillation amplitude of the two-link model, but increases the frequency.

Future work to observe what effects viscoelasticity might have on the flagellar beat of microscopic swimmers could involve expanding the two-link to consider other variables. For example, increasing the number of links, to make a three-link model or greater, may account for the greater amount elasticity a flagella has. Another idea is increasing the number of joined links in the plane itself to represent multiple filaments or microorganisms in close proximity within the fluid and how specific oscillation patterns change the effects of viscoelasticity.

References

[1] De Canio G, Lauga E, Goldstein RE. *Spontaneous oscilations of elastic filaments induced by molecular motors.* J. R. Soc. Interface 14: 20170491. http://dx.doi.org/10.1098/rsif.2017.0491

[2] Purcell E. M. *Life at low Reynolds number.* 1976, *Physics and Our World: A Symposium in Honor of Victor F. Weissnopf.* American Institute of Physics.

[3] Özkaya N, et al. *Fundamentals of Biomechanics: Equilibrium, Motion, and Deformation.* 2012, Springer Science and Business Media, LLC. DOI 10.1007/978-1-4614-1150-5,15